AN EXTENDED COMPLEX FINITE DIFFERENCE METHOD FOR THE ANALYSIS OF SEMICONDUCTOR LASERS WITH ELECTRODE DISCONTINUITIES

Shuoqi Chen and Ruediger Vahldieck

Laboratory for Lightwave Electronics, Microwaves and Communications (LLiMiC)
Department of Electrical and Computer Engineering, University of Victoria
Victoria, B.C., Canada V8W 3P6

ABSTRACT

The complex finite difference method is extended to form a self-consistent 3-D analysis tool for gain- and index- guided semiconductor lasers. Single- and double-strip laser diodes with and without strip discontinuities (to accommodate the bias current contact pad) are investigated by directly discretizing the 3-D Laplace equation, the 2-D carrier rate equation and the scalar wave equation. In combination with the Rayleigh variational principle, the complex propagation constant of the first two lowest order laser modes can be calculated as well as the complex refractive index distribution in the active layer.

INTRODUCTION

Semiconductor laser diodes are modulated at higher and higher bit rates requiring modulating bandwidths in excess of 30 GHz. Considering the low input impedance of most gain- and index-guided strip lasers, such a wide frequency range imposes serious matching problems for the microwave feed network. The situation becomes even worse due to the fact that laser diodes are insufficiently characterized at frequencies higher than 10-15GHz. Most laser diodes are represented by network models for which the element values are derived from either measurements or simple transmission line calculations. However, since a laser diode is basically an active transmission line, simple transmission line theory represents only a very rough approximation. On the other hand numerical techniques that have been developed for passive transmission lines can be utilized provided a self-consistent model including the Laplace and the carrier continuity equation can be developed.

If the laser diode is only regarded as a 2-D discontinuity, meaning that there is no longitudinal change in the refractive index or in the strip electrode, this problem has been largely solved [1]-[6]. For cases, however, in which the bias current contact pad is wider than the strip electrode, the 2-D model will not be valid anymore since now a 3-D distribution of the current and carrier density distribution must be taken into account. These changes in longitudinal direction affect the laser mode profile as well as the RF characteristics of the device.

In this paper we present a 3-D self-consistent numerical approach for a separate confinement heterostructure (SCH) strip laser with strip discontinuities along the longitudinal direction. This technique is based on the complex finite difference method[4][5] and takes into account the complex refractive index in the active layer which is a function of the bias current. The important feature here is that the imaginary part of the refractive index represents optical gain or loss which, in gain-guided lasers, is a function of the location of the electrode. For any calculation of the complex impedance of the laser diode, the transverse distribution of the complex gain profile must be known.

In the following we provide a brief description of the numerical algorithm to analyze SCH semiconductor lasers with single and twin strip electrodes containing discontinuities in longitudinal direction of the biasing electrode. Mode profiles as a function of the biasing current in twin strip lasers will be presented as well as the complex propagation constant and the current and carrier distribution at the interface of the active region.

WE 3F

THEORY

Fig. 1 shows the typical semiconductor lasers configuration with a separate confinement heterostructure. A slab waveguide structure is formed with an active waveguiding region sandwiched by two cladding layers. In the lateral direction there is no well-defined guiding structure. Weak waveguiding is provided by the lateral refractive index profile due to the injection current spreading from the passive cladding layer into the active layer. When a biasing voltage is applied to the strip, the potential distribution in the passive cladding layer can be found as a solution to

CH3577-4/95/0000-0805$01.00 © 1995 IEEE

Laplace's equation [5]:

$$\nabla^2 V = 0 \tag{1}$$

The current density injected into the active waveguiding layer can be obtained by using the following expression:

$$J|_{y=d} = -\sigma \cdot \nabla V|_{y=d} \tag{2}$$

Where d is the interface between the p-cladding and active layer. This injected current density acts as the source of the injected carrier distribution in the active layer. For large forward biasing, continuity of the majority carrier quasi-Fermi potential and charge neutrality condition can be assumed, because of very high carrier concentration in this region [6]. Along the lateral direction of the device the injected carrier density profile in the active region is described by the carrier rate equation which may be written as follows [4]:

$$D_{eff}\nabla^2 n - Bn^2 - \frac{c}{n_0} g S_0 \Psi + \frac{J}{qt} = 0 \tag{3}$$

where we assume $\partial n/\partial t = 0$ (steady-state condition). D_{eff} is the effective diffusion constant, n the local carrier density, B the carrier recombination constant, c the speed of light in free space, n_0 the background refractive index of the active region. g the gain profile across the active region, q the electronic charge, t the active layer thickness, J the local injected current density, S_0 the average photon density in the optical cavity, and Ψ the normalized optical intensity which may be defined as:

$$\Psi(x,y) = \frac{|E(x,y)|^2}{\iint |E(x,y)|^2 dxdy} \tag{4}$$

Equation (3) assumes that the active layer thickness t is small compared to the carrier diffusion length. This means that no recombination occurs outside the active region. Equations (1)~(3) are then solved self-consistently by using the complex finite difference method [5].

The field profile and propagation constant β can be obtained by solving the scalar wave equation which can be written as [3]:

$$\nabla_T^2 E + (k^2{}_0 n^2(x,y) - \beta^2) E = 0 \tag{5}$$

where ∇_T^2 is the transverse operator, β is the propagation constant, $n(x,y)$ is the local refractive index which exhibits a complex profile in the active region, and $k_0=2\pi/\lambda_0$ with λ_0 the free space wavelength of operation. In the implementation of the complex finite difference method the wave equation (5) can be written in five-point finite difference form to produce an expression for the field at each mesh point in terms of its four nearest neighbors. Each mesh point lies at the center of a cell of constant refractive index and changes in refractive index occur only at the cell boundaries. An iteration method is used to solve for the mesh point field values $E(i,j)$ and the propagation constant β which is found from a Rayleigh variational principle form [3][4]:

$$\beta^2 = \frac{\iint [E\nabla_T^2 E + k_0^2 n^2(x,y) E^2] dxdy}{\iint E^2 dxdy} \tag{6}$$

In this method an initial guess is made for β and the field value at each mesh point. Equations (5) and (6) are applied alternately. Each field value is updated and after each scan a new value of β is found. This process is continued until the solution for the mesh point field values and eigenvalue β converge. Note that the complex refractive indices are used directly in equations (5) and (6) producing a complex propagation constant and complex field values. This makes possible the straightforward application of the complex finite difference algorithm to active optical waveguide devices and semiconductor lasers with complex refractive indices in the active waveguiding region [4].

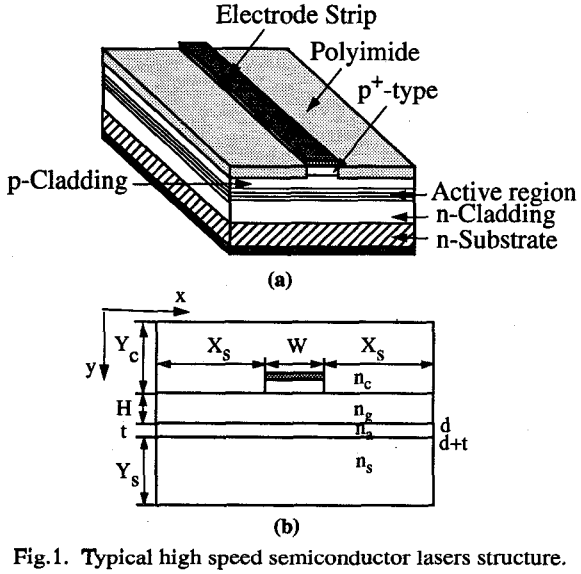

Fig.1. Typical high speed semiconductor lasers structure.

NUMERICAL RESULTS

To test the algorithm presented we first analyze a single-strip semiconductor laser with a discontinuity in the electrode structure. A biasing voltage of V_s=1.58V is applied to the electrode. The injected current density and carrier density profile along the active region is displayed

in Fig. 2 (a) and (b). The numerical analysis shows clearly that, as expected, in the region where the strip widens the carrier density is higher than in the narrower strip region. This results in a higher refractive index and consequently higher local gain in the active waveguiding region. This will have a direct effect on the mode confinement factor.

To demonstrate the flexibility of the algorithm we analyze next a semiconductor gain-guided laser with a slab waveguide structure. The 2D field profile for the fundamental scalar mode is shown in Fig. 3 (single-strip slab waveguide) and Fig.4 (twin-strip slab waveguide), respectively (W=3 μm, H=1 μm and G=3 μm (for twin-strip)). The refractive indices used are n_c=1, n_g=n_s=3.40 at an operating wavelength of 1.50 μm. The refractive index in the active region, but outside the area of the injected current, is normally a real value of n_a=3.44. Inside the area through which the injected current flows n_a is complex, whereby real and imaginary parts change in lateral direction. The mesh sizes used to discretize the structure are 0.05 and 0.2 μm in the x- and y-directions, respectively. A total of 10500 mesh cells is used. Fig. 3 clearly shows that the field is concentrated in the active waveguiding region under the strip with a bias voltage applied. For an asymmetrically pumped twin strip laser (two different biasing voltages applied), the gain-guiding region will shift towards the strip with the larger biasing voltage. This is shown in Fig. 4 and illustrates the beam steering capability of this structure.

The algorithm developed here provides the complex propagation constant and field profile for the fundamental and first order modes. Both are functions of the injected current into the active layer. With a biasing voltage Vs=1.6V, the single-strip laser structur in Fig.3 has a complex propagation constant of β_{eff}=3.40255+j3.61193x10^{-4}, and the twin-strip laser structure in Fig.4 β_{eff}=3.40452+j9.42884x10^{-4} (the biasing voltages are Vs1=1.65V and Vs2=1.6V). The real part of β_{eff} represents the normal propagation constant. The positive imaginary part indicates the optical gain for the wave propagating in the medium. A negative imaginary part indicates loss and occurs only outside the gain medium region. Comparing the two structures, the twin-strip laser requires larger bias and shows a higher imaginary β_{eff} value than that of the single-strip laser, which means also higher optical gain.

Semiconductor lasers with dielectric ridge and rib waveguide structures can also be analyzed with the approach developed here. First, we consider the ridge waveguide lasers. The 2D field profile of the fundamental scalar mode is shown in Fig. 5 (a) and (b) for the operating wavelength 1.50μm, where n_g=n_s=3.17 and n_a=3.34. At the biasing voltage of Vs=1.60V, we have β_{eff}=3.1952+j9.5242x10^{-4}.

The 2D field profile of the rib waveguide laser is shown in Fig. 6 (a) and (b) for the fundamental scalar mode operating at 1.50μm, where n_g=n_s=3.17 and n_a=3.34. At a biasing voltage of Vs=1.60V, we have β_{eff}=3.1967+j1.0538x10^{-3}. It is obvious that for these two index-guiding configurations the optical field is more confined in the wave guiding region compared to the gain-guided laser. At the same time, they have also higher values of the imaginary part of β_{eff} compared to the gain-guided laser.

CONCLUSIONS

We have presented a 3D self-consistent complex finite difference approach to analyze SCH semiconductor lasers with non-uniform strip geometry. Current and carrier distribution along the active layer of a variety of semiconductor laser structures have been calculated as well as their propagation constant and mode profiles. It was shown that electrode discontinuities can significantly change the complex refractive index in the active layer, which in turn may change the mode profile of the fundamental lasing mode. On the basis of this work a more accurate high frequency description of the laser diode is possible.

REFERENCES

[1] M.S. Stern: 'Semivectorial polarised finite difference method for optical waveguides with arbitrary index profiles', IEE Proc. J, vol.135, (1), pp. 56-63, 1988.

[2] M. Koshiba, H. Saitoh, M. Eguchi and K. Hirayama: 'Simple scalar finite element approach to optical rib waveguides', IEE Proc. J, vol.139, (2), pp. 166-171, 1992.

[3] M.A. Matin, T.M. Benson, P.C. Kendall and M.S. Stern: 'New technique for finite difference analysis of optical waveguide problems', International Journal of Numerical Modelling, vol.7, pp. 25-33, 1994.

[4] T.M. Benson, R.J. Bozeat and P.C. Kendall: 'Finite difference analysis of Active optical waveguide devices', IEE Second International Conference on Computation in Electromagnetics, 1994, pp.162-165.

[5] T. Kumar, R.F. Ormondroyd and T.E. Rozzi: 'A self-consistent model of the lateral behavior of a twin-stripe injection laser' IEEE J. Quantum Electron., vol. 22, (10), pp. 1975-1985, 1986.

[6] S.M. Lee, S.L. Chuang, R.P. Bryan, C.A. Zmudzinski and J.J. Coleman: 'A self-consistent model of a non-planar quantum-well periodic laser array', IEEE J. Quantum Electron., vol. 27, (7), pp. 1886-1899, 1991.

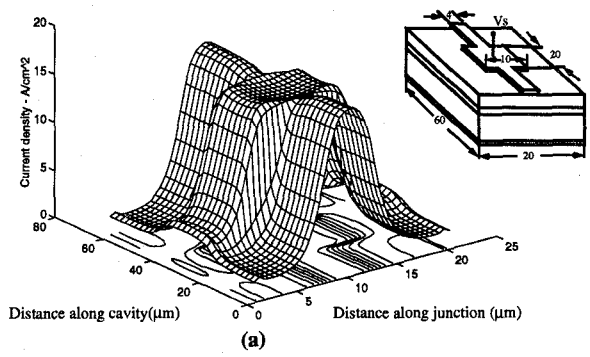

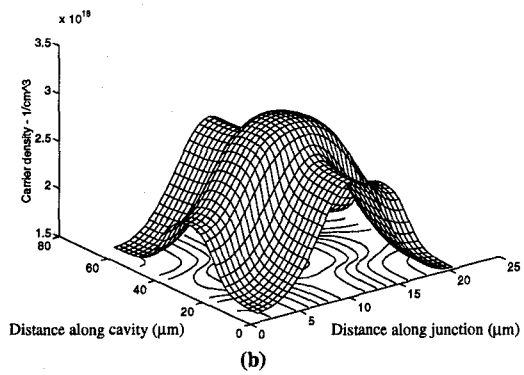

Fig.2 Semiconductor lasers with strip discontinuity (a) the injected current density distribution; (b) the injected carrier concentration profile in the active waveguiding region (biasing voltage V_s=1.58 V).

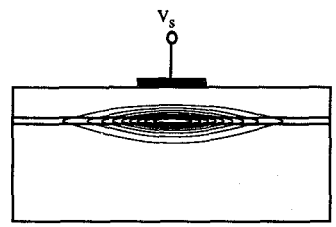

Fig.3 Two-dimensional field profile for the fundamental scalar mode within the semiconductor gain-guided laser diode with V_{s1}=1.6 V. Contour levels are at 10% intervals of the maximum field.

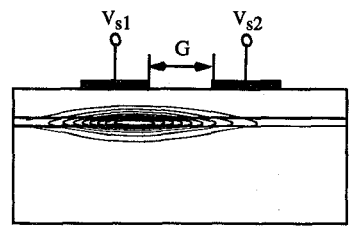

Fig.4 Two-dimensional field profile for the fundamental scalar mode within the semiconductor gain-guided laser diode with V_{s1}=1.65V, V_{s2}=1.6V. The effect of beam steering is clearly visible. Contour levels are at 10% intervals of the maximum field.

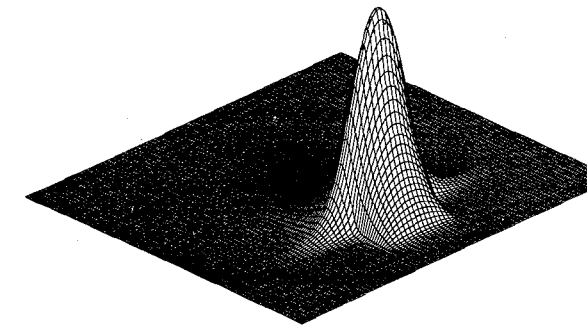

Fig.5 (a) The fundamental field distribution within the ridge waveguide semiconductor laser. (λ=1.50μm)

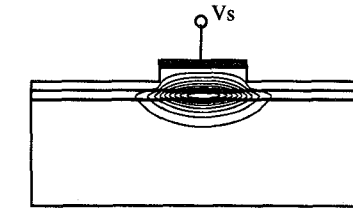

Fig.5 (b) Two-dimensional field profile for the fundamental scalar mode within a ridge waveguide semiconductor laser. Contour levels are at 10% intervals of the maximum field amplitude.

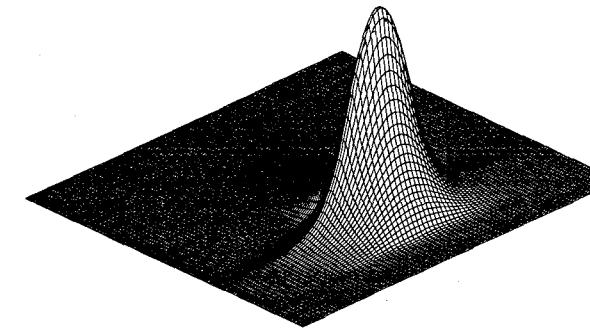

Fig.6 (a) The fundamental field distribution within the rib waveguide structure semiconductor laser. (λ=1.50μm)

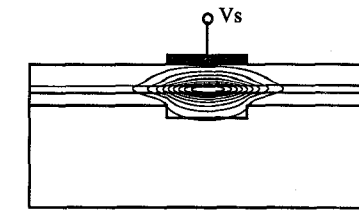

Fig.6 (b) Two-dimensional field profile for the fundamental scalar mode within the rib waveguide semiconductor laser. Contour levels are at 10% intervals of the maximum field amplitude.